

# Topological edge states in two-dimensional $\mathbb{Z}_4$ Potts paramagnet protected by the $\mathbb{Z}_4^{\times 3}$ symmetry

Hrant Topchyan,<sup>1</sup> Tigran Hakobyan,<sup>1,2</sup> Mkhitar Mirumyan,<sup>1</sup> Tigran A. Sedrakyan,<sup>1,3</sup> and Ara Sedrakyan<sup>1</sup>

<sup>1</sup>*A. Alikhanyan National Science Laboratory (Yerevan Physics Institute), Yerevan 0036, Armenia*

<sup>2</sup>*Yerevan State University, Yerevan 0025, Armenia*

<sup>3</sup>*Department of Physics, University of Massachusetts, Amherst, Massachusetts 01003, USA*

We construct a two-dimensional bosonic symmetry-protected topological (SPT) paramagnet protected by an on-site  $G = \mathbb{Z}_4^{\times 3}$  symmetry, starting from a three-component  $\mathbb{Z}_4$  Potts paramagnet on a triangular lattice. Within the group-cohomology framework,  $H^3(G, U(1)) \cong \mathbb{Z}_4^{\times 7}$ , we focus on a “colorless” cocycle representative obtained by antisymmetrizing the basic  $\mathbb{Z}_4$  three-cocycle, and generate the corresponding SPT Hamiltonian via a cocycle-induced nonlocal unitary transformation followed by symmetry averaging. For open geometry, we derive the boundary theory explicitly: one color sector decouples, while the nontrivial edge reduces to an interacting  $\mathbb{Z}_4$  chain with next-to-nearest-neighbor constraints that admits a compact dressed-Potts form. Using DMRG we show that the boundary model is gapless, with the lowest gap scaling as  $1/L$  and an entanglement-entropy scaling consistent with a conformal field theory of central charge  $c = 2.191(4) \simeq 11/5$ . The rational value  $c = 11/5$  matches the coset  $SU(3)_3/SU(2)_3$ , making it a candidate for the continuum description of the  $\mathbb{Z}_4^{\times 3}$  edge; we outline spectral and symmetry-resolved diagnostics needed to test this identification at the level of conformal towers beyond the central charge.

## I. INTRODUCTION

The structure of quantum states of matter at zero temperature has become a central theme in condensed-matter physics, motivated in part by rapid advances in quantum science and technology [1, 2]. A key lesson is that the classical Landau framework—based on spontaneous symmetry breaking and local order parameters—does not exhaust the possible organizing principles of quantum phases [3, 4]. In particular, two gapped ground states may remain in distinct phases even when they can be smoothly connected without breaking any symmetry, provided that they differ in their underlying topological structure.

Symmetry-protected topological (SPT) phases are among the simplest examples of such non-Landau quantum matter. They are short-range entangled, gapped phases whose distinction is stable only in the presence of a protecting on-site global symmetry [5–12]. Once the protecting symmetry is explicitly broken, different SPT phases can be adiabatically connected to a trivial product state without closing the bulk gap. Topological insulators [13, 14] and the Haldane spin-1 chain [15] provide canonical examples.

A defining property of an SPT phase is the constrained dynamics at its boundary. While the bulk can be fully gapped and nondegenerate, a symmetry-preserving boundary generically cannot be both gapped and nondegenerate: it must either remain gapless, spontaneously break the symmetry, or develop intrinsic topological order. This obstruction is captured by an anomalous realization of the symmetry at the boundary, i.e. the boundary symmetry cannot be implemented as a strictly on-site unitary action. Equivalently, the bulk admits a symmetry-protected topological response whose anomaly inflow cancels the boundary anomaly [16, 17].

The anomaly thus provides a sharp bulk invariant and underlies the bulk–boundary correspondence.

For bosonic systems with on-site symmetry  $G$  in  $d$  spatial dimensions, the group-cohomology construction classifies a large family of SPT phases by  $H^{d+1}(G, U(1))$  [16, 18]. In  $d = 1$ , the classification reduces to projective representations that appear at the ends of an open chain [19, 20]. In  $d = 2$ , the anomaly can be viewed as a failure of strict associativity of the symmetry action on the boundary; it is naturally exposed in the fusion of symmetry defect lines and is encoded by a three-cocycle in  $H^3(G, U(1))$ , often written in terms of  $F$ -symbols [21, 22]. Related viewpoints connect certain SPT models to intrinsically topologically ordered phases by duality transformations [23].

Recently, both the conceptual and practical toolkits for boundary anomalies have expanded substantially. On the conceptual side, generalized (including non-invertible and subsystem) symmetries and their symmetry topological field theory and topological-holography descriptions provide a unifying language for anomalies, gapped boundaries, and (intrinsically) gapless symmetry-protected phases [24–32]. On the practical side, systematic analyses of symmetry-preserving boundary conditions in CFT and refined numerical diagnostics of boundary anomalies continue to sharpen the bulk-boundary correspondence [33–38].

Concrete realizations of bosonic SPT phases via exactly solvable Hamiltonians with commuting local terms include decorated domain-wall constructions [39], cluster models [19, 40], the Levin-Gu model [23] for  $Z_2$  symmetry, and its generalizations to many-body states [41–43] and  $\mathbb{Z}_3^{\times 3}$  and  $\mathbb{Z}_3$  symmetries [44–46]. Related decorated-defect ideas have also been adapted to construct gapless SPT phases with protected boundary signatures [47].

In the seminal work [23], Levin and Gu showed that the nontrivial  $(2+1)$ -dimensional bosonic  $Z_2$  SPT ad-

mits no symmetry-preserving trivially gapped edge. Instead, the boundary degrees of freedom can be captured by a critical one-dimensional XX spin chain, i.e. the gapless point of the XY model. For the  $\mathbb{Z}_3$  and  $\mathbb{Z}_3^{\times 3}$  cases, Refs. [44–46] constructed exactly solvable bulk Hamiltonians and derived effective boundary Hamiltonians. In the continuum, the low-energy edge theory was argued to be described by the coset CFT  $SU_k(3)/SU_k(2)$  at level  $k$ . Numerical analysis suggested that the  $\mathbb{Z}_3$  edge corresponds to  $k = 1$ , while the  $\mathbb{Z}_3^{\times 3}$  edge corresponds to  $k = 2$ .

In this work, we extend the construction of Refs. [44–46] to the paramagnetic  $\mathbb{Z}_4^{\times 3}$ -symmetric Potts model on a triangular lattice and derive the associated effective boundary Hamiltonian. We then study its spectrum and entanglement properties to identify the emergent boundary CFT data.

## II. THE $\mathbb{Z}_4^{\times 3}$ SPT MODEL

In this section, we study the paramagnetic Potts model on a triangular lattice where the sites' states are given by the elements of the threefold product of the cyclic group of order four,

$$G = \mathbb{Z}_4^{\times 3} = \mathbb{Z}_4^A \times \mathbb{Z}_4^B \times \mathbb{Z}_4^C. \quad (1)$$

Here,  $\alpha \in \{A, B, C\}$  in the “color” index associated with the first, second, and third cyclic groups within the product, respectively.

Then the elements of group  $G$  can be given as 3-vectors with integer components (additive representation) and the group operation is the component-wise addition by modulo 4:

$$\begin{aligned} \mathbf{n} &= (n^A, n^B, n^C) \in G \text{ with } n^\alpha \in \{0, 1, 2, 3\}, \\ \mathbf{n}_1 + \mathbf{n}_2 &= \{n_1^\alpha + n_2^\alpha \pmod{4}\}. \end{aligned} \quad (2)$$

The lattice can be constructed from a three-colored triangular lattice with four-state sites by merging  $\nabla$ -type triangular faces into single composite sites in a specific way, as illustrated in Fig. 1. Then the on-site state of the constructed lattice is labeled by the integral vectors (2). For a given color  $\alpha$ , one can define operators

$$\begin{aligned} X|n\rangle &= |n - 1 \pmod{4}\rangle, \quad Z|n\rangle = i^n|n\rangle, \\ XZ &= iZX, \quad X^4 = Z^4 = 1. \end{aligned} \quad (3)$$

The operators at different points commute.

The noninteracting (paramagnetic) Potts model, which we use as the base for SPT phase construction, is described by the Hamiltonian

$$H_0 = - \sum_p \sum_\alpha \left( X_p^\alpha + (X_p^\alpha)^2 + (X_p^\alpha)^3 \right), \quad (4)$$

where the first sum is performed over the sites  $p$  of the constructed lattice and the second is over colors  $A, B, C$ .

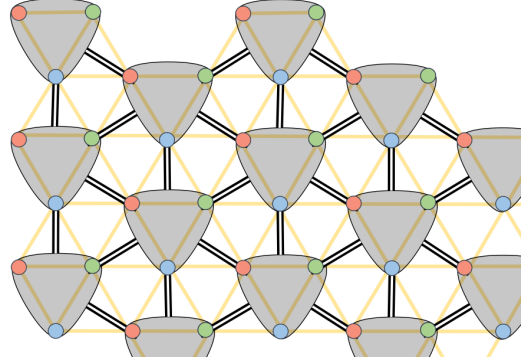


FIG. 1. The initial  $\mathbb{Z}_4$  triangular lattice with colored (red, green blue) nodes and yellow links and the colorless composite  $\mathbb{Z}_4^{\times 3}$  triangular lattice with gray-shaded triangles as the nodes and the black double line links.

The system (4) has a global symmetry  $G$  in representation  $S_g$  ( $\mathbf{g} \in G$ ),

$$[H_0, S_g] = 0, \quad S_g = \prod_p \prod_\alpha (X_p^\alpha)^{g^\alpha}. \quad (5)$$

### A. General structure of the SPT phase space

According to general theory, the nontrivial SPT phases of two-dimensional models are classified by the nontrivial elements of the third  $U(1)$  cohomology of the symmetry group. In our case, the latter is the sevenfold product of the underlying cyclic group [48]:

$$H^3(\mathbb{Z}_4^{\times 3}, U(1)) = \mathbb{Z}_4^{\times 7}. \quad (6)$$

The  $k$ -th cohomology group is defined as the factor of  $k$ -“cocycles” (or closed forms) to  $k$ -“coboudaries” (or trivial forms).  $k$ -cocycles and  $k$ -coboundaries of a group  $G$  are the  $G$ -invariant functions (cochains, forms)  $\nu_k : G^{\times (k+1)} \rightarrow U(1)$ ,  $\nu_k(g_0, \dots, g_k) = \nu_k(g + g_0, \dots, g + g_k)$  that obey conditions  $\delta\nu_k = 1$  and  $\nu_k = \delta\nu_{k-1}$ , respectively. Here,  $\delta : \nu_{k-1} \rightarrow \nu_k$  is the “coboundary” operator, which is defined in a way to exhibit a structure analogous to that of the standard exterior derivative of differential forms. Similarly, it is also nilpotent:  $\delta^2\nu_k = 1$ . The relevant expression of  $\delta$  is

$$\delta\nu_3(\mathbf{n}_0, \dots, \mathbf{n}_4) = \prod_{i=0}^4 \nu_3^{(-1)^i}(\mathbf{n}_0, \dots, \check{\mathbf{n}}_i, \dots, \mathbf{n}_4) \quad (7)$$

where notation  $\check{\mathbf{n}}_i$  indicates that the  $i$ -th argument is omitted. Using the  $G$ -invariance, one can eliminate the first argument of the form, yielding an alternative representation

$$\omega_3(\mathbf{n}_1, \mathbf{n}_2, \mathbf{n}_3) = \nu_3(0, \mathbf{n}_1, \mathbf{n}_1 + \mathbf{n}_2, \mathbf{n}_1 + \mathbf{n}_2 + \mathbf{n}_3), \quad (8)$$

$$\delta\omega_3(\mathbf{n}_1, \dots, \mathbf{n}_4)$$

$$= \frac{\omega_3(\mathbf{n}_2, \mathbf{n}_3, \mathbf{n}_4)\omega_3(\mathbf{n}_1, \mathbf{n}_2 + \mathbf{n}_3, \mathbf{n}_4)\omega_3(\mathbf{n}_1, \mathbf{n}_2, \mathbf{n}_3)}{\omega_3(\mathbf{n}_1 + \mathbf{n}_2, \mathbf{n}_3, \mathbf{n}_4)\omega_3(\mathbf{n}_1, \mathbf{n}_2, \mathbf{n}_3 + \mathbf{n}_4)}. \quad (9)$$

The relations (7), (8), and (9) extend naturally to arbitrary dimensions. Consequently, the closedness condition  $\delta\omega_3 = 1$  can be verified directly. In contrast, establishing the exactness condition is more subtle. In [44], it was established that if the 3-cocycle is trivial ( $\omega_3 = \delta\omega_2$  for some 2-cochain  $\omega_2$ ) then it satisfies the equation

$$R[\omega_3] := \prod_{\sigma \in \mathbb{S}_3} \omega_3^{\epsilon(\sigma)}(\mathbf{n}_{\sigma_1}, \mathbf{n}_{\sigma_2}, \mathbf{n}_{\sigma_3}) \xrightarrow{\omega_3 = \delta\omega_2} 1 . \quad (10)$$

Here, the product runs over all permutations  $\sigma = \{\sigma_1, \sigma_2, \sigma_3\} \in \mathbb{S}_3$  of the set  $\{1, 2, 3\}$  and  $\epsilon(\sigma) = \pm 1$  is the parity of the permutation  $\sigma$ .

## B. Construction of nontrivial SPT phases

The nontrivial SPT phases are described by Hamiltonians obtained from the original model (4) by a non-local unitary transformation generated by nontrivial 3-cocycles  $\nu_3 \in H^3(G, U(1))$  with subsequent symmetrization over the symmetry group  $G$  [40, 44–46, 49]:

$$\begin{aligned} H &= \frac{1}{|G|} \sum_{\mathbf{g} \in G} S_{\mathbf{g}} U H_0 U^\dagger S_{\mathbf{g}}^\dagger , \\ U &= \prod_{\langle pqr \rangle} \nu_3^{\epsilon(pqr)}(0, \mathbf{n}_p, \mathbf{n}_q, \mathbf{n}_r) , \end{aligned} \quad (11)$$

where the product is taken over all triangular faces of the composite lattice. The sign factor  $\epsilon_{\langle pqr \rangle} = \pm 1$  differentiates the triangle orientations:  $\epsilon = 1$  for the triangles pointing left ( $\triangleleft$ ) and  $\epsilon = -1$  for those pointing right ( $\triangleright$ ).  $|G| = 64$  is the order of the symmetry group (1).

Without the symmetrization procedure in (11),  $H_0$  and  $H$  would be unitarily equivalent. This is also the case for a closed system, even with symmetrization, as  $[S_{\mathbf{g}}, U] = 0, g \in G$  as a result of  $\delta\nu_3 = 0$  [45]. In the general case of an open system  $[S_{\mathbf{g}}, U] \neq 0$ , but rather  $S_{\mathbf{g}} U = V_{\partial, \mathbf{g}} U S_{\mathbf{g}}$  where  $V_{\partial, \mathbf{g}}$  are some terms on the system's boundary links (which makes it trivial on a closed system as  $\partial = \emptyset$ ). The averaging procedure over  $G$  in (11) is meant to restore the broken symmetry. If one separates the bulk ( $B$ ) and boundary ( $\partial$ ) sectors of the Hamiltonians,  $H_0 = H_{0,B} + H_{0,\partial}$ ,  $H = H_B + H_\partial$ , since  $[S_{\mathbf{g}}, H_0] = 0$  and by definition  $[V_{\partial, \mathbf{g}}, H_{0,B}]$ , then  $H_B$  will be  $U H_{0,B} U^\dagger$  while  $H_\partial$  will contain additional terms  $V_{\partial, \mathbf{g}}$  compared to  $U H_{0,\partial} U^\dagger$ . It is also apparent that  $[H_B, H_\partial] = 0$  [45, 49].

Let us now return to the cohomology group (6) of the considered model, which consists of seven independent  $\mathbb{Z}_4$  generators. The corresponding generators are well known and their color structure has been identified (see [50] as an example). Among these, there is a single “colorless”  $\mathbb{Z}_4$  element generated by the cocycle

$$\omega_3^o(\mathbf{n}_1, \mathbf{n}_2, \mathbf{n}_3) = i^{n_1^A n_2^B n_3^C} . \quad (12)$$

Its closedness can be verified directly and nontriviality is confirmed using (10) by verifying that, for instance,

$$R[\omega_3^o]((1, 0, 0), (0, 1, 0), (0, 0, 1)) = i \neq 1 . \quad (13)$$

$\omega_3^o$  is a representative of the cocycle class that corresponds to some element  $q$  of the factor (cohomology) group, and specifically the “colorless” component (direct factor)  $\mathbb{Z}_4$ . It is easy to show that  $q$  is the generator of that group: obviously,  $\delta(\omega_3 \omega_3^o) = \delta\omega_3 \delta\omega_3^o$  (7) and  $R[\omega_3 \omega_3^o] = R[\omega_3] R[\omega_3^o]$  (10).  $(\omega_3^o)^2$  and  $(\omega_3^o)^3$ , which correspond to the group elements  $q^2$  and  $q^3$ , respectively, are thus nontrivial cocycles as well. Since all  $q$ ,  $q^2$  and  $q^3$  are nontrivial,  $q$  is the generator of the cohomology group component  $\mathbb{Z}_4$ , and the different degrees of  $\omega_3^o$  cover the whole space of substantially different cocycles.

In this article, we consider a derived cohomology element obtained by antisymmetrizing (12) over its last two arguments:

$$\omega_3^a(\mathbf{n}_1, \mathbf{n}_2, \mathbf{n}_3) = i^{n_1^A (n_2^B n_3^C - n_2^C n_3^B)} . \quad (14)$$

The closedness condition  $\delta\omega_3^a = 1$  is easily verified, and the sufficient condition for the cocycle to be nontrivial  $R[\omega_3^a] \neq 1$  can be easily checked by evaluation with the same arguments as in (13). Moreover, one can check that the counterpart  $\omega_3^c = i^{-n_1^A n_2^C n_3^B}$  that was added to  $\omega_3^o$  belongs to the same cohomology as  $\omega_3^o$  itself ( $\omega_3^c \equiv \omega_3^o$ ). Indeed,  $\omega_3^o / \omega_3^c = \delta\omega_2$  with  $\omega_2(\mathbf{n}_1 \mathbf{n}_2) = i^{n_1^A n_2^B n_2^C}$ . Thus  $\omega_3^a = \omega_3^o \omega_3^c \equiv (\omega_3^o)^2$ , so  $\omega_3^a$  represents the order-two element of the “colorless” cohomology component  $\mathbb{Z}_4$ .

The corresponding invariant cocycle can be reconstructed using the relation (8):

$$\begin{aligned} \nu_3(0, \mathbf{s}, \mathbf{x}, \mathbf{y}) &= \omega_3^a(\mathbf{s}, \mathbf{x} - \mathbf{s}, \mathbf{y} - \mathbf{x}) = i^{\psi_3(\mathbf{s}, \mathbf{x}, \mathbf{y})} \\ \text{with } \psi_3(\mathbf{s}, \mathbf{x}, \mathbf{y}) &= s^A [x^B y^C - x^C y^B \\ &\quad - s^B (y^C - x^C) + s^C (y^B - x^B)] . \end{aligned} \quad (15)$$

## C. The boundary model

Let us apply the general expression of the SPT Hamiltonians (11) to this particular cocycle. Note that the exponent  $\psi_3$  in (15) is antisymmetric with regard to the permutation of its last two arguments, so

$$\nu_3(0, \mathbf{s}, \mathbf{x}, \mathbf{y}) = \nu_3(0, \mathbf{s}, \mathbf{y}, \mathbf{x})^{-1} . \quad (16)$$

This condition is required in order for the edge Hamiltonian to be translation-invariant and independent of the specific shape of the edge [45].

$$\begin{aligned} H_\partial &= -\frac{1}{64} \sum_s \sum_{p \in \partial, \alpha} V_{\mathbf{s}, p} \left( X_p^\alpha + (X_p^\alpha)^2 + (X_p^\alpha)^3 \right) V_{\mathbf{s}, p}^{-1} \\ \text{with } V_{\mathbf{s}, p} &= \frac{\nu_3(0, -\mathbf{s}, \mathbf{n}_p, \mathbf{n}_{p-1})}{\nu_3(0, -\mathbf{s}, \mathbf{n}_p, \mathbf{n}_{p+1})} . \end{aligned} \quad (17)$$

One may observe that any terms of the form  $f_{\mathbf{s}}(\mathbf{x})/f_{\mathbf{s}}(\mathbf{y})$  appearing in  $\nu_3(0, -\mathbf{s}, \mathbf{x}, \mathbf{y})$  cancel out in (17), so such terms can be omitted from the outset. More precisely, if there is  $\nu'(0, -\mathbf{s}, \mathbf{x}, \mathbf{y}) = \nu(0, -\mathbf{s}, \mathbf{x}, \mathbf{y}) \cdot f_{\mathbf{s}}(\mathbf{x})/f_{\mathbf{s}}(\mathbf{y})$ , then the corresponding  $V'_{\mathbf{s}, p} = V_{\mathbf{s}, p} \cdot f_{\mathbf{s}}(\mathbf{n}_{p+1})/f_{\mathbf{s}}(\mathbf{n}_{p-1})$ .

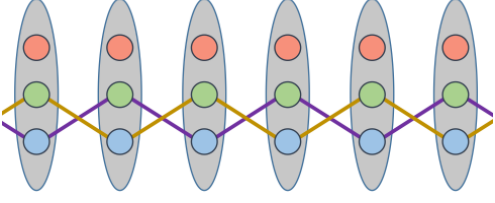


FIG. 2. The schematic depiction of interactions. The gray-shaded blobs are the lattice edge points, with their internal components of colors A (red), B (green) and C (blue). The interacting components are connected by brown or purple lines.

The additional terms are commutative with  $X_p^\alpha$ , so they vanish in the transformation  $V_{s,p}(\dots)V_{s,p}^{-1}$ , thus allowing for such  $\nu \rightarrow \nu'$  substitutions for the purpose of deriving  $H_\partial$ .

The expressions (15) are then simplified to

$$\nu'_3(0, -\mathbf{s}, \mathbf{x}, \mathbf{y}) = i^{-s^A(x^B y^C - x^C y^B)}. \quad (18)$$

Using the definition (3), it is straightforward to verify the relations

$$Z_p = i^{n_p}, \quad X_p^\alpha i^{n_p^\beta} = i^{n_p^\beta + \delta_\alpha^\beta} X_p^\alpha, \quad \sum_{s=0}^3 i^{ks} = 4\delta_k^{(4)},$$

where  $\delta^{(N)}$  denotes the Kronecker delta modulo  $N$ ,  $\delta_k^{(N)} = \delta_{k \bmod N}$ . Then the similarity transformations in the expression for the edge Hamiltonian (17) reduce the local terms as follows:

$$(X_p^A)^k \rightarrow (X_p^A)^k, \quad (19)$$

$$(X_p^B)^k \rightarrow \frac{1}{4}(X_p^B)^k \sum_{s=0}^3 (Z_{p-1}^C Z_{p+1}^C)^{ks} = (X_p^B)^k \delta_{k \Delta n_p^C}^{(4)},$$

$$(X_p^C)^k \rightarrow \frac{1}{4}(X_p^C)^k \sum_{s=0}^3 (Z_{p-1}^B Z_{p+1}^B)^{ks} = (X_p^C)^k \delta_{k \Delta n_p^B}^{(4)}.$$

where we introduced the notations  $\Delta n_p^\alpha = n_{p+1}^\alpha - n_{p-1}^\alpha$ .

The boundary Hamiltonian  $H_\partial$  contains next-to-nearest neighbor interactions, schematically shown in Fig.2. One can see a trivial separation of the color A and the splitting of the remaining terms into two distinct  $\mathbb{Z}_4$  chains, each consisting of the colors B and C in alternating order. This occurs when the edge has even length; otherwise, the seemingly separate chains combine into a single chain that is twice as long.

Using the relations  $\delta_{2n}^{(4)} = \delta_n^{(2)}$  and  $\delta_{3n}^{(4)} = \delta_n^{(4)}$  for Kronecker deltas to simplify the local terms (19), one can acquire the Hamiltonian of a single  $\mathbb{Z}_4$  chain in the form

$$\tilde{H}_\partial = - \sum_p \left[ (X_p + X_p^\dagger) \delta_{\Delta n_p}^{(4)} + X_p^2 \delta_{\Delta n_p}^{(2)} \right], \quad (20)$$

with  $\Delta n_p = n_{p+1} - n_{p-1}$ . The color labels disappear at this stage, since we now deal with a single  $\mathbb{Z}_4$  chain rather than a  $\mathbb{Z}_4^{\times 3}$  system. The tilde in  $\tilde{H}_\partial$  indicates that it is only the nontrivial part of  $H_\partial$ .

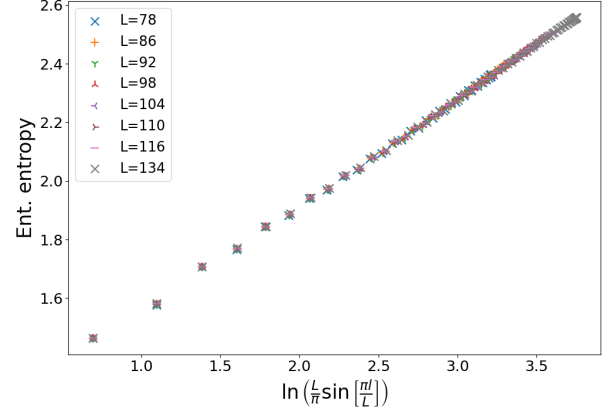


FIG. 3. The entanglement entropy on reparameterized subsystem size ratio  $l/L$  for various system sizes  $L$ . Central charge  $c = 2.191 \pm 0.004$  can be determined from the slope.

### III. NUMERICAL ANALYSIS OF THE BOUNDARY MODEL

The edge Hamiltonian (17) can be presented in a simple form

$$\begin{aligned} \tilde{H}_\partial = & -\frac{1}{4} \sum_p \left[ X_p + Z_{p-1}(X_p + X_p^\dagger)Z_{p+1}^\dagger \right. \\ & \left. + X_p^2 + Z_{p-1}^2(X_p + X_p^2)Z_{p+1}^{\dagger 2} + \text{h.c.} \right]. \end{aligned} \quad (21)$$

According to [51], the entanglement entropy in a conformal field theory with central charge  $c$  on an open system of length  $L$  is given by

$$S_L(l) = a + \frac{c}{6} \ln \left( \frac{L}{\pi} \sin \left[ \frac{\pi l}{L} \right] \right), \quad (22)$$

where  $l$  is the length of the considered subsystem and  $a$  is some constant. For a closed system, the coefficient  $c/6$  in front of the log should be replaced by  $c/3$ . This formula defines the finite-size behavior of entanglement entropy in a chain model at criticality. It allows to obtain the value of the central charge  $c$  through numerical calculations.

Running DMRG (which is used in this study) on periodic chains for this edge model is much more costly in term of computational resources (both the runtime and memory requirements) compared to the equivalent calculations on open chains. Here we have concentrated on an open chain to be able consider a longer chain and reach desirable precision.

The data in Fig.3 shows the numerically obtained values of entanglement entropy versus the rescaled subsystem size  $l$ ,  $\ln(\frac{L}{\pi} \sin[\frac{\pi l}{L}])$  for various  $L = 78, 86, 92, 98, 104, 110, 116, 134$  for an open chain. We see a perfectly straight line for all  $L$ -s in agreement with (22), from which the values of parameters  $c = 2.191 \pm 0.004 \simeq 11/5$  and  $a = 1.186$  are obtained.

We then analyze the spectrum of low-energy modes of the derived boundary Hamiltonian to check for gapless excitations, which are a prerequisite for describing

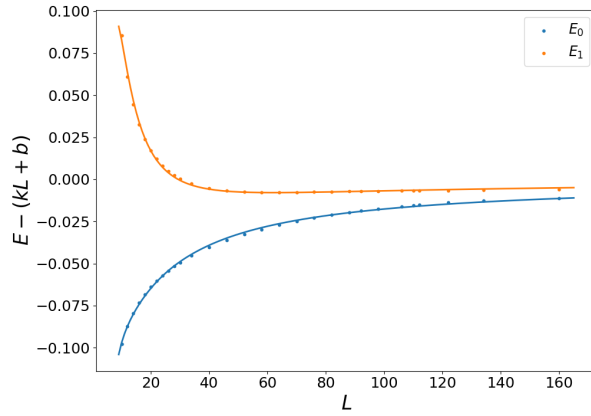


FIG. 4. The ground state energy  $E_0$  and the first excited state energy  $E_1$  on system size  $L$ , after subtracting the linear term in  $L$ . The numerical results (dots) and the corresponding fitting curves.  $h_1^{(b)} = (0.019 \pm 0.009)c$ .

the system within a conformal field theory paradigm. The DMRG simulations of the edge Hamiltonian provide strong evidence that the boundary theory is indeed gapless.

Fig.4 displays the ground state energy  $E_0$  and the first excited state energy  $E_1$  versus the system size  $L$  for open chains. According to [34, 52–54] the finite-size behavior of the lower energy states read as

$$\begin{aligned} E_0(L) &= kL + b - \frac{\pi v c}{24L} + \mathcal{O}(L^{-2}), \\ E_i(L) &= E_0(L) + \frac{\pi v}{L} h_i^{(b)} + \mathcal{O}(L^{-2}), \end{aligned} \quad (23)$$

where  $k, b, v$  are some constants,  $c$  is the central charge and  $h_i^{(b)}$  are the *boundary* scaling dimensions (a single chiral sector) set by the conformal boundary conditions of the microscopic edge. The decomposition into bulk weights  $(h_i, \bar{h}_i)$  and the momentum quantization  $P \propto (h_i - \bar{h}_i)$  apply to periodic chains.

Excitation gap defined as the energy difference between the first excited state and the ground state—as a function of system size  $L$ ,  $\Delta_1^{(b)} = E_1 - E_0$ . One can see that the finite-size gap decreases steadily as  $L$  grows

$$\Delta_1^{(b)} \simeq \frac{\pi v h_1^{(b)}}{L}. \quad (24)$$

Fitting the numerical data for  $E_0(L)$  and  $E_1(L)$  by the functions (23) and using the values for the central charge  $c = 2.191 \pm 0.004$ , we have obtained the numerical value for the smallest boundary scaling dimension accessible in the open-chain spectrum via DMRG within the symmetry sector to be  $h_1^{(b)} = 0.04 \pm 0.02$ , within the available precision. Directly extracting the bulk weights  $(h, \bar{h})$  and the momentum quantization  $P \propto (h_i - \bar{h}_i)$  requires periodic boundary conditions and momentum resolution. The presented calculations have been done for an open system of sizes  $L = 10 \sim 160$ .

Motivated by the  $Z_3$  and  $Z_3^{\times 3}$  SPT edges [44, 46], it is natural to ask whether the present  $Z_4^{\times 3}$  edge criticality is also described by coset CFT  $SU_k(3)/SU_k(2)$  at some level  $k$ . A particularly suggestive possibility is at  $k = 3$ , since the numerically extracted central charge  $c = 2.191 \pm 0.004$  is close to the rational value  $11/5$ .

For the Wess-Zumino-Novikov-Witten models one has

$$c(SU(N)_k) = \frac{k(N^2 - 1)}{k + N}, \quad (25)$$

$$c_{\text{coset}}(k) = c(SU(3)_k) - c(SU(2)_k) = \frac{8k}{k + 3} - \frac{3k}{k + 2}.$$

Setting  $k = 3$  gives  $c_{\text{coset}}(3) = 11/5$ , which agrees with our entanglement entropy estimate within the numerical precision. This is strong evidence that low-energy edge theory is compatible with the  $SU(3)_3/SU(2)_3$  coset.

The definitive identification, however, requires matching the operator content based on the conformal towers[55], not only  $c$ . Our preliminary open-chain estimate for the *boundary* scaling dimension in a single chiral sector, determined by the conformal boundary conditions of the microscopic edge, is  $h_1^{(b)} = 0.04 \pm 0.02$ . It does not obviously coincide with one of the simplest values quoted above. This may reflect a finite-size effect, a symmetry-sector restriction in DMRG computation, or the specific conformal boundary condition realized by  $\tilde{H}_\partial$ . Therefore, to sharpen the CFT identification beyond the central charge, one will need to: (i) extract several low-lying gaps (and degeneracies) in symmetry-resolved sectors and match them to conformal towers, (ii) perform smaller-size periodic-boundary calculations to access both energies and momenta, enabling a direct extraction of bulk  $(h, \bar{h})$ , and (iii) analyze correlators and/or the entanglement spectrum to identify the leading lattice operators and their scaling dimensions. Since decomposition into true bulk weights  $(h_i, \bar{h}_i)$  and momentum quantization  $P \propto (h_i - \bar{h}_i)$  apply to periodic chains, a better computer infrastructure will be required to compute these.

#### IV. CONCLUSION

We have studied  $Z_4^{\times 3}$  Potts model in paramagnetic phase and constructed one set of its seven  $Z_4^7$  SPT phases defined by the cohomology group  $H^3(Z_4^{\times 3}, U(1)) = Z_4^{\times 7}$ . In particular, we focused on the diagonal action of the symmetry, where each site of the triangular lattice hosts three Potts variables—each transforming under a different copy of  $Z_4$ . Using this setup, we explicitly constructed the corresponding  $Z_4$  cocycles that generate all SPT phases of  $Z_4$ . More precisely, we focused on the antisymmetrized  $\omega_3^a$  in Eq. (14), which is designed to satisfy the antisymmetry constraint Eq. (16) needed for a shape-independent edge Hamiltonian. As indicated by  $R[\omega_3^a] = -1$ , this representative is naturally interpreted as an order-two element within the “colorless”  $Z_4$  factor, and extending the construction to a full set of seven

independent generators of  $H^3(\mathbb{Z}_4^{\times 3}, U(1))$  (and to other order-four representatives) is left for future work.

We have also formulated a gapless edge state chain model with symmetry  $Z_4$ , which is a hallmark of nontrivial SPT phase. Numerically we found the central charge of this edge states  $c \simeq 11/5$  and the boundary scaling dimension in a single chiral sector  $h_1^{(b)} \approx 0.04$ . Our central charge estimate is compatible with the  $SU(3)_3/SU(2)_3$  coset CFT, which has an exact  $c = 11/5$ . Verifying the continuum theory beyond the central charge involves a systematic comparison of the low-energy spectrum with the expected conformal towers, including symmetry-

resolved sectors and degeneracies, and ideally additional periodic-boundary data. Finally, since our gap analysis is based on an open chain, the exponent we find should be considered a boundary scaling dimension; identifying  $(h, \bar{h})$  in the bulk requires periodic spectra with momentum resolution.

## ACKNOWLEDGMENTS

The authors acknowledge Armenian HESC grants 24RL-1C024 (HT, TS), 21AG-1C024 (MM, AS), 24FP-1F039 (TH, HT, AS), and 21AG-1C047 (TH) for financial support.

---

[1] B. Zeng, X. Chen, D.-L. Zhou, and X.-G. Wen, *Quantum Information Meets Quantum Matter: From Quantum Entanglement to Topological Phases of Many-Body Systems*, 1st ed., Quantum Science and Technology (Springer, New York, NY, 2019).

[2] S. Sachdev, *Quantum Phases of Matter* (Cambridge University Press, 2023).

[3] L. D. Landau, On the theory of phase transitions, *Zh. Eksp. Teor. Fiz.* **7**, 19 (1937).

[4] L. Landau and L. E.M., *Statistical Physics. Vol. 5* (Elsevier Science, 2013).

[5] Z.-C. Gu and X.-G. Wen, Tensor-entanglement-filtering renormalization approach and symmetry-protected topological order, *Phys. Rev. B* **80**, 155131 (2009).

[6] T. Senthil, Symmetry-protected topological phases of quantum matter, *Annual Review of Condensed Matter Physics* **6**, 299 (2015).

[7] X.-G. Wen, Colloquium: Zoo of quantum-topological phases of matter, *Rev. Mod. Phys.* **89**, 041004 (2017).

[8] F. Pollmann, E. Berg, A. M. Turner, and M. Oshikawa, Symmetry protection of topological phases in one-dimensional quantum spin systems, *Phys. Rev. B* **85**, 075125 (2012).

[9] F. Pollmann, A. M. Turner, E. Berg, and M. Oshikawa, Entanglement spectrum of a topological phase in one dimension, *Phys. Rev. B* **81**, 064439 (2010).

[10] X. Chen, Z.-C. Gu, and X.-G. Wen, Local unitary transformation, long-range quantum entanglement, wave function renormalization, and topological order, *Phys. Rev. B* **82**, 155138 (2010).

[11] L. Fidkowski and A. Kitaev, Topological phases of fermions in one dimension, *Phys. Rev. B* **83**, 075103 (2011).

[12] N. Schuch, D. Pérez-García, and I. Cirac, Classifying quantum phases using matrix product states and projected entangled pair states, *Phys. Rev. B* **84**, 165139 (2011).

[13] M. Z. Hasan and C. L. Kane, Colloquium: Topological insulators, *Rev. Mod. Phys.* **82**, 3045 (2010).

[14] X.-L. Qi and S.-C. Zhang, Topological insulators and superconductors, *Rev. Mod. Phys.* **83**, 1057 (2011).

[15] F. D. M. Haldane, Nonlinear field theory of large-spin heisenberg antiferromagnets: Semiclassically quantized solitons of the one-dimensional easy-axis n\'eel state, *Phys. Rev. Lett.* **50**, 1153 (1983).

[16] X. Chen, Z.-C. Gu, Z.-X. Liu, and X.-G. Wen, Symmetry-protected topological orders in interacting bosonic systems, *Science* **338**, 1604 (2012).

[17] G. 't Hooft, Naturalness, chiral symmetry, and spontaneous chiral symmetry breaking, *NATO Sci. Ser. B* **59**, 135 (1980).

[18] X. Chen, Z.-C. Gu, Z.-X. Liu, and X.-G. Wen, Symmetry protected topological orders and the group cohomology of their symmetry group, *Phys. Rev. B* **87**, 155114 (2013).

[19] X. Chen, Z.-C. Gu, and X.-G. Wen, Classification of gapped symmetric phases in one-dimensional spin systems, *Phys. Rev. B* **83**, 035107 (2011).

[20] X. Chen, Z.-C. Gu, and X.-G. Wen, Complete classification of one-dimensional gapped quantum phases in interacting spin systems, *Phys. Rev. B* **84**, 235128 (2011).

[21] K. Kawagoe and M. Levin, Anomalies in bosonic symmetry-protected topological edge theories: Connection to  $f$  symbols and a method of calculation, *Phys. Rev. B* **104**, 115156 (2021).

[22] J. Maeda and T. Oishi, N-ality symmetry and SPT phases in (1+1)d, *JHEP* **12**, 063, arXiv:2504.20151 [hep-th].

[23] M. Levin and Z.-C. Gu, Braiding statistics approach to symmetry-protected topological phases, *Phys. Rev. B* **86**, 10.1103/physrevb.86.115109 (2012).

[24] R. Thorngren and Y. Wang, Fusion category symmetry. part I. Anomaly in-flow and gapped phases, *JHEP* **2024** (04), 132, arXiv:1912.02817 [hep-th].

[25] N. Seiberg, S. Seifnashri, and S.-H. Shao, Non-invertible symmetries and LSM-type constraints on a tensor product Hilbert space, *SciPost Phys.* **16**, 154 (2024), arXiv:2401.12281 [hep-th].

[26] L. Bhardwaj, L. E. Bottini, D. Pajer, and S. Sch\"afer-Nameki, Gapped phases with non-invertible symmetries: (1+1)d, *SciPost Phys.* **18**, 032 (2025), arXiv:2310.03784 [hep-th].

[27] A. Antinucci, C. Copetti, and S. Sch\"afer-Nameki, SymTFT for (3+1)d gapless SPTs and obstructions to confinement, *SciPost Phys.* **18**, 114 (2025), arXiv:2408.05585 [hep-th].

[28] Q. Jia and Z. Jia, Subsystem symmetry-protected topological phases from subsystem SymTFT of 2-foliated exotic tensor gauge theory, *JHEP* **2025** (09), 170,

arXiv:2505.22261 [hep-th].

[29] N. Seiberg, S.-H. Shao, and W. Zhang, LSM and CPT, JHEP **2025** (11), 116, arXiv:2508.17115 [hep-th].

[30] N. Seiberg and S. Seifnashri, Symmetry transmutation and anomaly matching, JHEP **09**, 014, arXiv:2505.08618 [hep-th].

[31] K. Wang and T. A. Sedrakyan, Universal finite-size scaling around tricriticality between topologically ordered, symmetry-protected topological, and trivial phases, Phys. Rev. B **101**, 035410 (2020).

[32] K. Wang and T. A. Sedrakyan, Universal finite-size amplitude and anomalous entanglement entropy of  $z = 2$  quantum Lifshitz criticalities in topological chains, SciPost Phys. **12**, 134 (2022).

[33] L.-Y. Li, Y.-T. Hsieh, Y. Yao, and M. Oshikawa, Boundary conditions and anomalies of conformal field theories in dimensions  $D \geq 3$ , Phys. Rev. B **110**, 045118 (2024).

[34] Y. Liu, H. Shimizu, A. Ueda, and M. Oshikawa, Finite-size corrections to the energy spectra of gapless one-dimensional systems in the presence of boundaries, SciPost Phys. **17**, 099 (2024).

[35] K. Ding, H.-R. Zhang, B.-T. Liu, and S. Yang, Boundary anomaly detection in two-dimensional subsystem symmetry-protected topological phases, Phys. Rev. B **111**, 205125 (2025), arXiv:2412.07563 [cond-mat.str-el].

[36] K. Loo and Q.-R. Wang, Systematic construction of interfaces and anomalous boundaries for fermionic symmetry-protected topological phases, Phys. Rev. B **111**, 205102 (2025), arXiv:2412.18528 [cond-mat.str-el].

[37] Y. Xu and C.-M. Jian, Average-exact mixed anomalies and compatible phases, Phys. Rev. B **111**, 125128 (2025), arXiv:2406.07417 [cond-mat.str-el].

[38] Y. Guo and S. Yang, Strong-to-weak spontaneous symmetry breaking meets average symmetry-protected topological order, Phys. Rev. B **111**, L201108 (2025), arXiv:2410.13734 [cond-mat.str-el].

[39] X. Chen, Y.-M. Lu, and A. Vishwanath, Symmetry-protected topological phases from decorated domain walls, Nature Communications **5**, 3507 (2014).

[40] B. Yoshida, Topological phases with generalized global symmetries, Phys. Rev. B **93**, 155131 (2016).

[41] T. A. Sedrakyan, V. M. Galitski, and A. Kamenev, Topological spin ordering via chern-simons superconductivity, Phys. Rev. B **95**, 094511 (2017).

[42] R. Wang, B. Wang, and T. Sedrakyan, Chern-simons superconductors and their instabilities, Phys. Rev. B **105**, 054404 (2022).

[43] R. Wang, B. Wang, and T. A. Sedrakyan, Chern-simons fermionization approach to two-dimensional quantum magnets: Implications for antiferromagnetic magnons and unconventional quantum phase transitions, Phys. Rev. B **98**, 064402 (2018).

[44] H. Topchyan, V. Iugov, M. Mirumyan, S. Khachatryan, T. Hakobyan, and T. Sedrakyan,  $\mathbb{Z}_3$  and  $(\times \mathbb{Z}_3)^3$  symmetry protected topological paramagnets, JHEP **2023** (12).

[45] H. Topchyan, SPT extension of  $\mathbb{Z}_2$  quantum ising model's ferromagnetic phase, Phys. Lett. A **517**, 129669 (2024).

[46] H. Topchyan, V. Iugov, M. Mirumyan, T. Hakobyan, T. A. Sedrakyan, and A. G. Sedrakyan, Two-dimensional topological paramagnets protected by  $\mathbb{Z}_3$  symmetry: Properties of the boundary Hamiltonian, SciPost Phys. **18**, 068 (2025).

[47] L. Li, M. Oshikawa, and Y. Zheng, Decorated defect construction of gapless-SPT states, SciPost Phys. **17**, 013 (2024), arXiv:2204.03131 [cond-mat.str-el].

[48] A. Mesaros and Y. Ran, Classification of symmetry enriched topological phases with exactly solvable models, Phys. Rev. B **87**, 155115 (2013).

[49] B. Yoshida, Gapped boundaries, group cohomology and fault-tolerant logical gates, Annals of Physics **377**, 387 (2017).

[50] M. de Wild Propitius, *Topological interactions in broken gauge theories*, Ph.D. thesis, - (1995), arXiv:hep-th/9511195 [hep-th].

[51] P. Calabrese and J. Cardy, Entanglement entropy and conformal field theory, Journal of Physics A: Mathematical and Theoretical **42**, 504005 (2009).

[52] H. W. J. Blöte, J. L. Cardy, and M. P. Nightingale, Conformal invariance, the central charge, and universal finite-size amplitudes at criticality, Phys. Rev. Lett. **56**, 742 (1986).

[53] J. L. Cardy, Operator content of two-dimensional conformally invariant theories, Nuclear Physics B **270**, 186 (1986).

[54] J. L. Cardy, Effect of boundary conditions on the operator content of two-dimensional conformally invariant theories, Nuclear Physics B **275**, 200 (1986).

[55] P. Di Francesco, P. Mathieu, and D. Senechal, *Conformal Field Theory* (Springer-Verlag, New York, 1997).